THINK INDIA JOURNAL

ISSN:0971-1260
Vol-22-Issue-37-December -2019

MicrostructureAssessment in LaserWeldment of SS-316L

Chandan Kumar[1], Manas Das[2], Hitesh Vasudev[3]

[1,3]*Lovely Professional University, Jalandhar, Department of Mechanical Engineering, Punjab*
[2]*Indian Institute of Technology Guwahati, Department of Mechanical Engineering, Assam*

Emails: [1]chandan.25012@lpu.co.in, [2]manasdas@iitg.ac.in, [3]hitesh.24804@lpu.co.in

Abstract

In the current research work, fiber laser welding of 0.5 mm thin SS-316L sheetsare performed. Feasibility study is conducted to find the suitability of welding of SS-316L material by fiber laser. The suitable parameters are selected from the beads on plate experiment which yield the full penetration in the actual welding experiment in butt shape. Crack free weld is achieved. The microstructural features areconducted under optical microscope.The fusion zone microstructure comprises of primarily austenite matrix with a very low amount of delta ferrite (δ) along the grain boundaries. The mechanical properties are tested by tensile test and its values are lesser than the parent material of SS-316L. The fractgraphy analysis reflects the ductile mode of fracture failure of the weldment.

Keywords*:Fiber Laser, Welding, SS-316L, Microstructure,Tensile Strength, Fractgraphy*

1. Introduction

Fibre laser weldingprocess possesses many benefits such as very high energy density, localized heating which yields smaller size of fusion zone(FZ) and heat affected zone (HAZ), low heat input, deeper penetration, high traverse speed, lesser distortion, high production, excellentquality of weldment, manufacturing flexibility, and high bead aspect ratio [1-4]. Lasers are highly suitable for welding SS-316L due to their low line energy and high traverse speed which reduces metallurgical defects and it enhances the strength of weldments [5, 6].Stainless steels are basically an iron alloy which contains at least 12% (by weight) chromium. Austenitic stainless steel has high level of nickel as well as chromium. During starting of 20th century, it wasfound that by adding Cr at least 12% in stainless steel, its corrosion resistance dramatically increases. Austenitic stainless steel of grade 316L is considered to be more resistant to corrosion due to its high concentration of chromium and nickel typically ranges between 18-20 % and 8-12 %, respectively [5-7]. Austenitic stainless steel has good ductility and strength which is maintained

Copyright ⓒ 2019Authors

ISSN:0971-1260
Vol-22-Issue-37-December -2019

alsoat lower temperature. It can be hardened by plastic deformation without embrittlement. Among all types of austenitic stainless steels, grade 316L (i.e. SS-316L) is mostly used in petrochemical, nuclear, marine, architectural applications, heat exchanger tubes, and corrosive chemical environments, aerospace and automotive industries [6-9].SS-316Lis not susceptible to solidification cracking during high speed laser beam welding process. The thermal conductivity of SS-316L is one-third of carbon steels and it has higher absorption coefficient. Hence, higher depth of penetration is achieved in case of SS-316L than carbon steel for the same experimental condition [9-12].

Benjamin et al.[13] did weld bead characterization of 8 mm thick SS-316L material by electron beam welding process by varying laser power. It was found that material hardness decreases with increasing Q/V ratio due to the variation in cooling rate. Q is heat energy and V is welding speed. Further, they found that material toughness is decreased by increasing Q/V ratio due to reduced grain size which depends on FZ cooling rate. Also, they found that ferrite concentration in FZ highly depends on cooling rate. Tadamalle et al. [14] reported that welding efficiency of Nd: YAG welded stainless steel of AISI 304L grade depends mostly on welding speed. Defect free weld can be obtained at optimum welding speed.Miranda et al. [15] compared microstructures of 19 mm thick low carbon steel plate welded using fiber laser and TIG. It was observed that the microstructure in the base metal is changed from fine-grain-ferrite and pearlite to fine-structure martensite after welding. With increased heat input, the microstructure in the fusion zone becomes coarser with Widmanstatten morphology with decreased hardness value. Fine microstructure was observed in TIG welding with lower hardness value than fiber laser in the fusion zone. Narrow and deep penetrations of weld bead, fine grain structure were observed in fiber laser than TIG welding of same material.Sathiya et al. [16] employed Taguchi approach to find out optimal welding condition and also to develop correlation between beam power, welding speed and defocused position with penetration depth, FZ width and tensile properties. The current study deals the microstructural evaluation in the FZ of SS-316L and it explore the change in mechanical properties of laser welded specimen in detail.

2. Experimentation

In this study, a 2000 Watt continuous wave (CW) ytterbium doped fibre laser is employed for experimentation. The fibre laser is a kind of solid state laser and its wavelength (λ)

Copyright ⓒ 2019Authors

ISSN:0971-1260
Vol-22-Issue-37-December -2019

is approximately 1.08 μm. The selected fibre laser iscontrollednumerically by CNC controller. The experimental setup used in this investigation is displayed in Fig. 1.The SS-316L thin sheet having dimensions 100 X 100 X 0.5 mm^3 is placed on a specifically fabricated fixture with protective gas carriage system and it is held by means of clamping device in order to reduce the warpage and movement of the sample for the period of the laser welding operation. The angle of incidence of laser beam with respect to vertical axis is selected as 85^0.The elemental constituents of SS-316L are presented in tabular form as depicted in Table 1

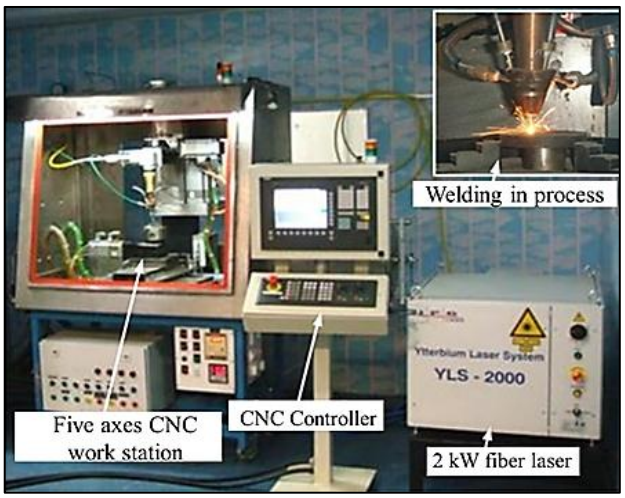


Fig. 1 Fiber laser welding setup

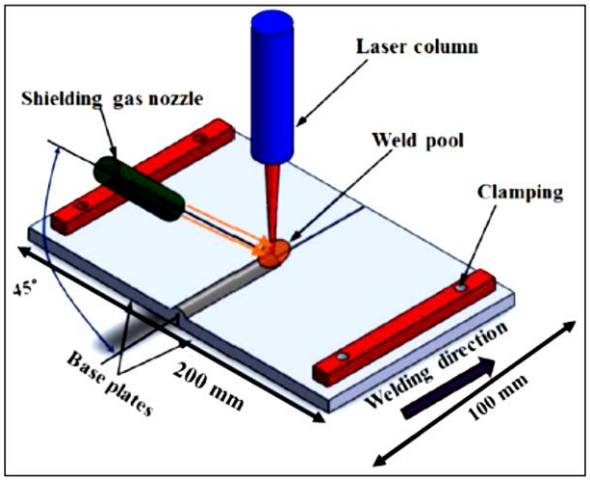


Fig. 2 Schematic diagram of fixture

Table 1 Chemical compositions of BM of SS-316L

Element	**C**	**Mn**	**P**	**S**	**Si**	**Cr**	**Ni**	**Mo**	**N**	**Fe**
Wt.%	0.03	0.9	0.1	0.3	1.7	17.3	9.5	1.6	0.1	Bal.

Copyright ⓒ 2019Authors

200 mm

ISSN:0971-1260
Vol-22-Issue-37-December -2019

Preliminary beads on plate experiments are conducted by employing fiber laser to perform the feasibility of welding of SS-316L sheets. The feasibility study reflects that the inert gas environment is essential during welding of SS-316L. Therefore, a fixture is designed in such a way that it can deliver the inert gas on bottom side of the weldments as shown in Fig. 2.Argon gas with less than 0.01 % impurities is used as a shielding gas. It helps to reduce the oxidation issue of the welded region. From the beads on plate experiment, the suitable parameters are identified as 550 Watt beam power and a traverse speed of 0.8 m/min. It yields full penetration in the sheets. Therefore, the welding in butt shape is carried out at this selected process parameters. For metallographic test weldments are cut by wire electro discharge machine and it is mounted on polishing wheel using resin to make the surface smooth.The specimens were etched with etchant (equal amount of HCl, HNO_3 and CH_3COOH). The morphological study of developed microstructure is carried out in optical microscope.The tensile test specimens are made as per ASTM E-8 standard [17]. The tensile test isconductedin Instron model machine with 10 KN load and for a constantcross-head speedi.e. 1.0 mm/min. Fractgraphy study is also conducted to explore the mode of fracture failure.

3. Results and Discussion

The microstructure evaluation in FZ and mechanical properties of weldment of SS-316L material is discussed in the following sub-section.

3.1 Macrograph of weld bead

Figure 3 shows the macrograph of fully penetrated fiber laser welded SS-316Lspecimenat 550 Watt power and a traverse speed of 0.8 m/min.

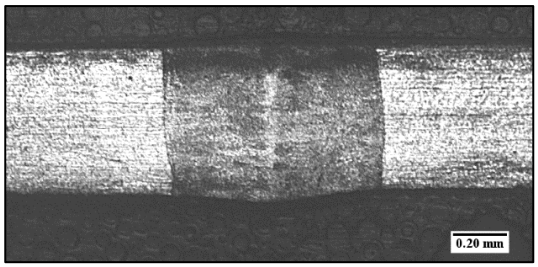


Fig. 3 Macrograph of fully penetrated weldment

The weldment is crack free and without any void. This is possible due to the high crack resisting property of the material and proper selection of welding parameters.In Fig. 3 shape of FZ cross-section are sandglass shape and the FZ width at upper and lower surfaces are nearly same due to

Copyright ⓒ 2019Authors

ISSN:0971-1260
Vol-22-Issue-37-December -2019

the development of open keyhole inside the melt pool. Due to high pressure in the keyhole, thermally activated gas can also eject out from both upper and bottom surfaces. Therefore, the FZ width at the upper and bottom are nearly same.Due to non-uniform temperature gradient in the workpiece material, three zones are observed in the weldments i.e. FZ, HAZ and base metal zone (BMZ) as depicted in optical image in Fig. 4.

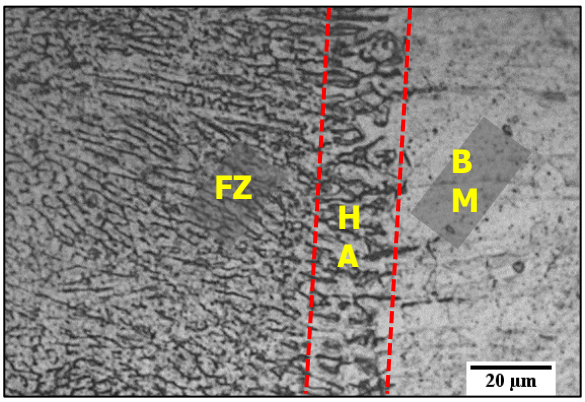


Fig. 4 Different zones in the weld bead

3.2 Microstructural Analysis

At ambient temperature, austenitic steel contains a mixture of austenite-ferrite structure. After welding the microstructure of FZ are changed. The fusion zone microstructure comprises of primarily austenite matrix with a very low amount of delta ferrite (δ) along the grain boundaries as depicted in Fig. 5.

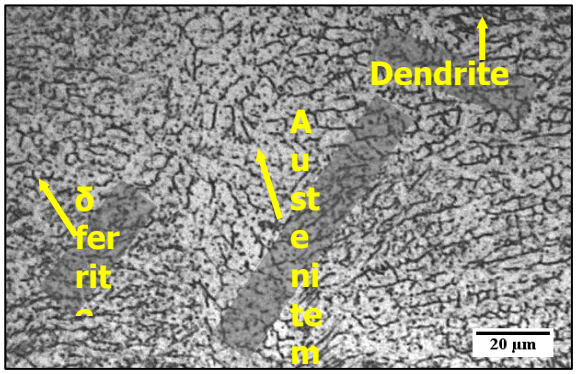


Fig. 5 Microstructure in fusion zone

The modes of solidification depend on the ratio of Cr_{eq}/Ni_{eq}. After solidification ofFZ, primary delta ferrite developed in this zone and then transformation of delta ferrite to austenite occurs. This solid state phase change is a diffusion controlled transformation. The extremely high

Copyright ⓒ 2019Authors

ISSN:0971-1260
Vol-22-Issue-37-December -2019

cooling rate of laser welding process doesn't provide the enough time to complete the transformation. Therefore, small amount to delta ferrite (δ) is still observed in the FZ.

3.3Tensile Test and Fractography

The tensile test results are shown in Table 2. It shows the strength and elongation of the welded specimen andparent metal of SS-316L. In case of fibre laser weldment, fracture occurs at the FZ and it has a lower value of strength in comparison withparent metal. It is probably due to the inefficient and insufficient delivery of the inert gas in the melt pool and the improper shape of the nozzle. The FESEM micrograph in Fig. 6, show the fracture surface of SS-316L weldment after tensile test. Cup shaped dimples of different sizes (Fig. 6) and with few tearing ridges are found in the fracture surface of weldment. It reveals the characteristics of fracture failure of weldment in ductile mode.

Table 2 Mechanical properties of parent metal and weldment

Sample specification	Yield strength (MPa)	Ultimate tensile strength (MPa)	% elongation
Parent metal	360.38	598.26	40.24
Weldment	318.62	546.28	28.66

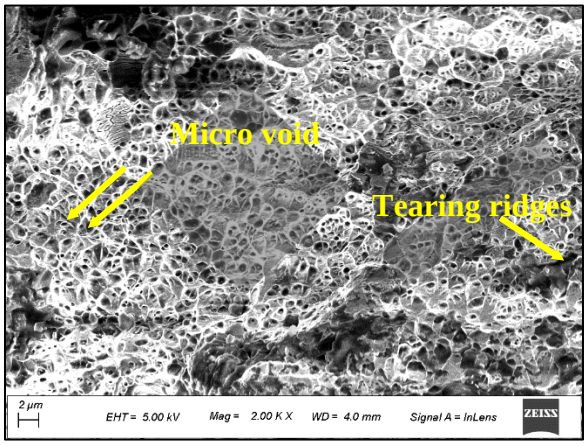


Fig. 6 Fracture surface of weldment

4. Conclusion

The fibre laser welding experiment is conducted on 0.5 mm thinSS-316L sheets. Smooth and crack free weld is formed. The weld beadsize is almost equal on both the upper and

Copyright ⓒ 2019Authors

ISSN:0971-1260
Vol-22-Issue-37-December -2019

bottomregion. The tensile strength and the elongation of the weldmentsare reduced after welding. It is probably due to both the inefficient and insufficient delivery of the argon gas in the welded region and also due to the improper design of shielding gas nozzle. The gas delivery system must be configured in such a way that the both front and back side of the welded zones are not in contact with the atmospheric gases.The fracture failure of the weldment occurs in ductile mode.

References

1. A. Costa, R. Miranda, L. Quintino, and D. Yapp, "Analysis of beam material interaction in welding of titanium with fiber lasers," Mater. Manuf. Process. vol. 22, pp. 798–803, 2007.
2. J. Ahn, L. Chen, C. M. Davies, and J. P. Dear, "Parametric optimisation and microstructural analysis on high power Yb-fibre laser welding of Ti–6Al–4V," Opt. Lasers Eng. vol. 86, pp. 156–171, 2016.
3. C. Kumar, M. Das, C. P. Paul, and Singh, B, "Experimental investigation and metallographic characterization of fiber laser beam welding of Ti-6Al-4V alloy using response surface method," Opt. Lasers Eng. vol. 95, pp. 52–68, 2017.
4. L. Quintino, A. Costa, R. Miranda, D. Yapp, V. Kumar, and C. J. Kong, "Welding with high power fiber lasers-A preliminary study," Mater. Des. vol. 28, pp. 1231-1237, 2007.
5. M. Sabzi, and S. M. Dezfuli, "Drastic improvement in mechanical properties and weldability of 316Lstainless steel weld joints by using electromagnetic vibration during GTAW process," J. Manuf. Process. vol. 33, pp. 74–85, 2018.
6. G. F. Sun, X. T. Shen, Z. D. Wang, M. J. Zhan, S. Yao, R. Zhou, and Z. H. Ni, "Laser metal deposition as repair technology for 316L stainless steel: Influence of feeding powder compositions on microstructure and mechanical properties," Opt. Laser Technol. vol. 109, pp. 71-83, 2019.
7. G. Chandrasekar, C. Kailasanathan, and M. Vasundara, "Investigation on un-peened and laser shock peened dissimilar weldments of Inconel 600 and AISI 316L fabricated using activated-TIG welding technique," J. Manuf. Process. vol. 35, pp. 466–478, 2018.
8. K. Hao, G. Li, M. Gao, X. Zeng, "Weld formation mechanism of fiber laser oscillating welding of austenitic stainless steel," J. Mater. Process. Technol. vol. 225, pp. 77–83, 2015.

Copyright ⓒ 2019Authors

ISSN:0971-1260
Vol-22-Issue-37-December -2019

9. M. Mukherjee, S. Saha, T.K.Pal, and P. Kanjilal, "Influence of modes of metal transfer on grain structure and direction of grain growth in low nickel austenitic stainless steel weld metals," Mater. Charact. vol. 102, pp. 9–18, 2015.
10. C. D'amato, M. Fenech, S. Abela, J.C. Betts, J. Buhagiar, Autogenous laser keyhole welding of AISI 316LTi. Mater. Manuf. Process. 25 (2010) 1269–1277.
11. J. C. Rahman, M.Vasudevan, S. Muthukumaran, R. K. Ravi, and N. Chandrasekhar,"Simulation of laser butt welding of AISI 316L stainless steel sheet using various heat sources and experimental validation," J. Mater. Process. Technol. vol. 219, pp. 48–59, 2015.
12. B. K. Joseph, D. Sathiya, P. Murthy, and C. V. Srinivasa, "Weld metal characterization of 316L(N) austenitic stainless steel by electron beam welding process", Int. J. Eng. Sci. Technol. vol. 4, pp. 169-176, 2012.
13. J. Benjamin, D. Katherasan, P. Sathiya, M. C. V. Srinivasa, "Weld metal characterization of 316L(N) austenitic stainless steel by electron beam welding process," Int. J. Engg. Sci. Technol. vol. 4, pp. 169-176, 2012.
14. A. P. Tadamalle, Y. P.Reddy, E.Ramjee, and V. Reddy, "Evaluation of Nd: YAG Laser Welding Efficiencies for 304L Stainless Steel,"Procedia Mater. Sci. vol. 6, pp. 1731–1739, 2014.
15. R. Miranda, A. Costa, L. Quintino, D. Yapp, and D. Iordachescu, "Characterization of fiber laser welds in X100 pipeline steel," Mater. Des. vol. 30, pp. 2701-2707, 2009.
16. P. Sathiya, M. Y. A. Jaleel, D. Katherasan, and B. Shanmugarajan, "Optimization of laser butt welding parameters with multiple performance characteristics," Opt. Laser Technol. vol. 43, pp. 660–673, 2011.
17. Standard test methods for tension testing of metallic materials ASTM E8 / E8M ASTM International, West Conshohocken, PA, 2013.

Copyright ⓒ 2019Authors